

A Regularised EEG Informed Kalman Filtering Algorithm



Shirin Enshaeifar*, Loukianos Spyrou*, Saeid Sanei* and Clive Cheong Took*

Abstract

The conventional Kalman filter assumes a constant process noise covariance according to the system's dynamics. However, in practice, the dynamics might alter and the initial model for the process noise may not be adequate to adapt to abrupt dynamics of the system. In this paper, we provide a novel informed Kalman filter (IKF) which is informed by an extrinsic data channel carrying information about the system's future state. Thus, each state can be represented with a corresponding process noise covariance, i.e. the Kalman gain is automatically adjusted according to the detected state. As a real-world application, we demonstrate for the first time how the analysis of electroencephalogram (EEG) can be used to predict the voluntary body movement and inform the tracking Kalman algorithm about a possible state transition. Furthermore, we provide a rigorous analysis to establish a relationship between the Kalman performance and the detection accuracy. Simulations on both synthetic and real-world data support our analysis.

Index Terms

Electroencephalogram, informed Kalman, voluntary movement prediction, state detection.

1 INTRODUCTION

KALMAN filtering (KF) is a popular state estimation technique which has found a wide range of applications in science and technology. It provides optimal error correction for noisy and inaccurately modelled random processes through a recursive algorithm which accumulates information regarding the process characteristics. Recently, the Kalman algorithm has been formulated in the quaternion domain representation to track in three-dimensional spaces [1], [2], [3].

The Kalman algorithm requires prior knowledge of the system such as the system model, its initial conditions and the noise characteristics to provide a robust performance. The conventional Kalman filter algorithm considers processes where the noise characteristics or the system dynamics remain stationary [2], [4]. However, those characteristics may change in their structure and behaviour, such as random system failures, environmental disturbances and abrupt variation of the operating point [5]. Thus, the conventional Kalman filter may not be able to capture those changes resulting in suboptimal performance. For instance, consider a motion tracking system where there are periods in which the motion dynamics are of either low or high variance. In this case, a stationary process noise model is not optimal [5], [6].

The performance of the Kalman filter depends on the Kalman gain, a parameter which provides a tradeoff between the actual observations and the model predictions. The Kalman gain is computed based on the noise characteristics and determines the performance of the KF. In a motion tracking system, a Kalman gain can be tuned to achieve noise reduction behaviour by assuming a low value and responsiveness by assuming a large value. Since the Kalman gain is directly affected by the process noise covariance, the correct estimation of this matrix can significantly enhance the robustness and reliability of the KF.

These problems have been addressed in [6], where a state-based gain adaptation algorithm was developed in which the Kalman gain depended on the observed measurements. However, in practice, online identification of the transition point is very challenging, especially when the data contain high level of noise. In this work, we propose an informed Kalman filter (IKF) algorithm where the Kalman gain is automatically updated based on an extrinsic data channel which provides information about the state of the system. Thus, optimal behaviour can be established for systems exhibiting non-stationary changes in the system model, its dynamics and in the noise behaviour. The external data channel operates as a predictor of the future evolution of the system's parameters and its prediction accuracy is critical for the IKF efficacy.

We demonstrate a practical application of the IKF algorithm by considering motion tracking of human arm movements and the extrinsic data channel corresponds to concurrent electroencephalography (EEG) measurements. An early indication of volitional movement is the pre-motor or readiness potential (RP), which appears about 0.5-1.5 seconds prior to the initiation of voluntary movement [7], [8], [9], [10].

The RP is known as part of the slow-wave motion related cortical potential (MRCP) which is related to the movement planning and execution. The RP wave is represented as a slow decrease in EEG amplitude starting about 1.5 seconds prior to the movement onset [7], [8] where the decreasing rate reaches a steep slope about 0.4 seconds before the movement, see Fig. 1.

*The authors are with the Department of Computing, University of Surrey, Surrey, GU2 7XH, UK.

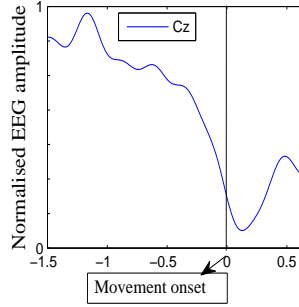


Fig. 1: The obtained readiness potential for a healthy subject. The RP wave is in agreement with literature [7].

Thus, we aim to detect the online RP prior to motion execution and impart it to the proposed IKF as the system change predictor. Note that online detection of the RP wave from single-trials has always been a challenge due to the poor signal to noise ratio (SNR) of the EEG [10]. Furthermore, the onset and appearance of the RP wave can differ among participants and movement conditions. This is due to several factors such as level of intention, preparatory state, speed and precision of movement, pace of movement repetition, complexity of movement, and pathological lesions of various brain structures [8]. In this work, we provided a uniform preparation state for subjects and they were asked to perform a similar arm movement. The RP wave was detected using an individual template-matching algorithm.

The design of the IKF in this work employs a quaternion representation for the motion tracking data but the same principles apply for real or complex data.

2 METHODOLOGY

Recently, Kalman filtering has been formulated within the quaternion domain to address 3-D altitude estimation problems [1]. Similar to the conventional KF, the quaternion KF is a recursive algorithm that consists of two major steps, prediction and update. The KF behaviour is often discussed in terms of \mathbf{K}_0 or Kalman gain, a correction factor for state estimation, which is affected by both process noise (\mathbf{Q}) and measurement noise (\mathbf{R}) matrices. Thus, optimising the system to have reasonable values for covariance matrices \mathbf{Q} and \mathbf{R} is required for optimal performance.

2.1 EEG informed Kalman gain

In this section, we introduce an informed Kalman algorithm in which the Kalman gain is adjusted according to the state of the system. Consider the system \mathbf{S}_r which represents a random mixture of low and high variance dynamics represented by two process noise covariances \mathbf{Q}_1 and \mathbf{Q}_2 respectively. For this system, \mathbf{Q}_2 is preferred when noise reduction is the main objective, while \mathbf{Q}_1 is applied for higher responsiveness of the KF to abrupt changes. Thus, we propose the IKF in which the combined gain leverages both of these performance advantages according to the state of the data. The gain is derived from \mathbf{K}_1 and \mathbf{K}_2 , thereby taking into account the noise statistics \mathbf{Q}_1 and \mathbf{Q}_2 , and a regularisation parameter α which reflects the state variance. In other words, α is defined such that \mathbf{K}_2 is the principal gain for low variance movements to denoise the data, while \mathbf{K}_1 is the primary gain for high variances, such as occurrence of sudden changes, to compensate for the delayed response. The derivation of the novel Kalman gain in terms of the system characteristics is included in Appendix-A.

In practice, online identification of the transition point is challenging, especially when the data contain high level of noise. Therefore, we assume that this instant is highly correlated with a known distinct feature in an extramural channel, such as RP wave in EEG before the movement execution. Thus, rather than the actual data, we exploit an extrinsic EEG channel (\mathbf{x}) to inform the KF for state recognition and gain adaptation. The IKF¹ is summarised in Algorithm 1.

Algorithm 1 Informed Kalman Filter

Initialisation of the Kalman variables

Kalman state prediction

$$\tilde{\mathbf{q}}_p(t+1) = \mathbf{F}\tilde{\mathbf{q}}_u(t)$$

$$\mathbf{P}_{p_i}(t+1) = \mathbf{F}\mathbf{P}_{u_i}(t)\mathbf{F}^T + \mathbf{Q}_i \quad i \in \{1, 2\}$$

$$\mathbf{K} = \alpha\mathbf{K}_1 + (1 - \alpha)\mathbf{K}_2 \quad \text{where} \quad \mathbf{K}_i = \mathbf{P}_{p_i}(t+1)\mathbf{H}^T(\mathbf{H}\mathbf{P}_{p_i}(t+1)\mathbf{H}^T + \mathbf{R})^{-1} \quad i \in \{1, 2\}$$

Kalman update

$$\tilde{\mathbf{q}}_u(t+1) = \tilde{\mathbf{q}}_p(t+1) + \mathbf{K}(\mathbf{q}_{os} - \mathbf{H}\tilde{\mathbf{q}}_p(t+1))$$

$$\mathbf{P}_{u_i}(t+1) = (\mathbf{I} - \mathbf{K}\mathbf{H})\mathbf{P}_{p_i}(t+1) \quad i \in \{1, 2\}$$

¹Throughout this paper, \mathbf{H} represents the observation model to map the state space into the observed space, and \mathbf{F} is a matrix of state model to illustrate the system's dynamic. The $\tilde{\mathbf{q}}_p$ and $\tilde{\mathbf{q}}_u$ are the priori (predict) and posteriori (update) states respectively and \mathbf{q}_{os} is the observed state.

Note that $0 \leq \alpha \leq 1$ is the regularisation factor. On one hand, $\alpha = 1$ provides maximum convergence and highest responsiveness, on the other hand $\alpha = 0$ is optimal for the low-variance state; and therefore $\alpha > 0$ models the transient state. In this work, the value of α is affected by detection of the RP which is achieved via a template matching obtained from the training EEG data.

3 IKF PERFORMANCE ANALYSIS

To analyse the performance of proposed IKF against noise, assume that for the system S_r , both Q covariance matrices are diagonal where $Q_1 > Q_2$. Theoretically, for small SNR, e.g. region (a) in Fig. 2, the noise reduction is more crucial than responsiveness and small Kalman gain leads to a lower error or E_2 . On the other hand, for high SNR, region (b) in Fig. 2, noise is less dominant and quick adaptation of the Kalman algorithm is desired. Thus, the error of high Kalman gain or E_1 is smaller.

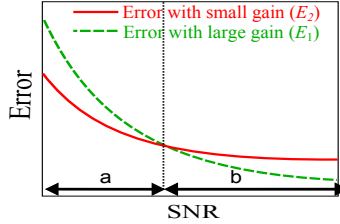


Fig. 2: Illustration of Kalman error vs. SNR for two different noise covariance matrices, where Q_1 (dotted line) $>$ Q_2 (solid line).

Using the proposed IKF, the objective is to leverage both of these performance advantages regardless of SNR, such that the performance shifts towards the optimal case. However in practice, the exterior predictor channel is noisy and this affects the state detection and consequently the IKF behaviour. Therefore, the IKF performance should be also examined in terms of detection accuracy of events in the predictor channel (EEG). For statistical analysis, a most common index of the accuracy is associated with a receiver operating characteristic (ROC) curve. This curve is acquired by plotting the true positive rate (TPR) versus false positive rate (FPR) for various detection thresholds [7]. In general, the final threshold is selected at the knee of the ROC curve so that there is a balance between TPR and FPR, see Fig. 3. Statistical measurements used in this work are summarised in Table I.

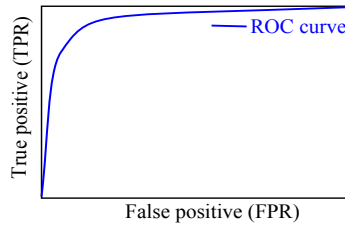


Fig. 3: Index of accuracy or ROC curve.

TABLE I: Statistical measurements

	Detection ON	Detection OFF
Jump execution	True positive (TP)	False negative (FN=1-TP)
Low variance	False positive (FP)	True negative (TN=1-FP)

In order to derive the expected IKF error in terms of the statistical parameters, consider the following cases in parallel with Fig. 2.

(1) Consider that $\alpha = 0$ and Kalman gain K_2 is based on Q_2		(2) Consider that $\alpha = 1$ and Kalman gain K_1 is based on Q_1	
Low SNR	High SNR	Low SNR	High SNR
The small gain is optimal, unless it switches to K_n for a false jump recognition. Hence, the error E_2 is directly related to FPR as	The default gain K_2 reduces the responsiveness. Thus, it can be improved by switching it to K_n for correct jump detections or TPR.	The high gain KF constantly tends to track the noise. Hence, we aim to switch it off during the low variance state which is defined as TNR in Table I.	The E_1 is optimal unless we miss a jump detection and turn it off by mistake. Thus, aggravation of E_1 is related to FNR.
$\tilde{E}_2 = E_2 + \text{FPR} E_2 - E_1 $	$\tilde{E}_2 = E_2 - \text{TPR} E_2 - E_1 $	$\tilde{E}_1 = E_1 - \text{TNR} E_2 - E_1 $	$\tilde{E}_1 = E_1 + \text{FNR} E_2 - E_1 $

Therefore, the final expected error \tilde{E}_{IKF} for each region can be approximated as the average of errors \tilde{E}_1 and \tilde{E}_2 :

$$\tilde{E}_{\text{IKF}} \simeq \frac{\tilde{E}_1 + \tilde{E}_2}{2} \begin{cases} \text{Region } a \begin{cases} \tilde{E}_2 = E_2 + \text{FPR} | E_2 - E_1 | \\ \tilde{E}_1 = E_1 - \text{TNR} | E_2 - E_1 | \end{cases} \\ \text{Region } b \begin{cases} \tilde{E}_2 = E_2 - \text{TPR} | E_2 - E_1 | \\ \tilde{E}_1 = E_1 + \text{FNR} | E_2 - E_1 | \end{cases} \end{cases} \quad (1)$$

Thus considering the optimal detection of events in the predictor channel (TPR=1 and FPR=0), \tilde{E}_{IKF} can be simplified as:

$$\tilde{E}_{\text{IKF}} \simeq \begin{cases} \text{mean}(E_2, E_1 - |E_2 - E_1|) = E_2 & \text{Region } a \\ \text{mean}(E_2 - |E_2 - E_1|, E_1) = E_1 & \text{Region } b \end{cases} \quad (2)$$

Note that for $0 < \alpha < 1$, value of \tilde{E}_{IKF} is expected to vary between E_1 and E_2 for both regions a and b .

4 EXPERIMENTAL RESULTS

To demonstrate the efficiency of our proposed method, IKF was evaluated on both synthetic and real-world data.

4.1 Synthetic data

The first experiment was carried out to evaluate the tracking accuracy for different levels of white Gaussian noise. To generate the synthetic data, first we modelled the default state by a quaternion autoregressive AR(4) process $\mathbf{q} = [q_1, \dots, q_N]$ where:

$$q_t = 0.9q_{t-1} - 0.7q_{t-2} + w_t \quad (3)$$

in which the driving noise was four-dimensional zero mean white Gaussian noise. Then, we randomly located 10 quadruple Gaussian functions ($\text{gauss}(\sigma_i, T_i)$) to simulate the arm movement in 3D space:

$$\mathbf{q} = \mathbf{q} + \sum_{i=1}^{10} \text{gauss}(\sigma_i, T_i) \quad (4)$$

where T_i defines the location of the i th Gaussian block. Note that each block had a random standard deviation σ_i selected from a uniformly distributed set. Furthermore, to generate the extrinsic channel on motion prediction, we considered a pulse signal prior to the Gaussian blocks. The pulses were randomly placed 50-150 samples ahead of the blocks to simulate the RP temporal condition. Overall, 30 sets of simulated data were generated to aggregate the results.

In order to evaluate the proposed method, recall the two prominent components that affect the IKF behaviour: (i) noise level and (ii) detection accuracy of the external predictor. To consider both parameters, first we adjusted the exterior channel to provide various TPR values (25%, 50%, 75% and 100%). Then, white Gaussian noise with different levels of SNR varying from -20dB to 20dB was added to each case. Performance of the proposed method was assessed in terms of the normalised root mean square error (NRMSE) between signal (\mathbf{q}) and the estimated ($\hat{\mathbf{q}}$). Hence, the lower the error, the better the system is.

$$\text{NRMSE} = \frac{\sqrt{\frac{\sum(\mathbf{q} - \hat{\mathbf{q}})^2}{N}}}{\max(\mathbf{q}) - \min(\mathbf{q})} \quad (5)$$

Fig. 4 represents the averaged NRMS error obtained from the proposed IKF and two conventional KF with different \mathbf{Q} matrices. Note that \mathbf{Q}_1 and \mathbf{Q}_2 were selected based on the variance of the noise-free dynamics.

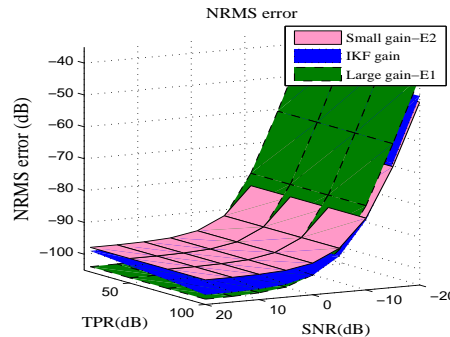


Fig. 4: The effect of SNR and TPR on the IKF performance compared with two basic KFs. The error was averaged over 30 sets of data.

This figure illustrates the averaged error against both prominent parameters TPR and SNR. It confirms that the detection accuracy is a key factor in IKF behaviour, such that higher TPR significantly improves the performance. Furthermore, Fig. 4 shows that for TPR=100%, IKF constantly provided the near-optimal performance regardless of the SNR values. In this experiment, FPR was considered as zero; however, in reality it is unlikely to have zero FPR for high TPR values.

4.2 Real-world EEG data

This section involves the results of applying IKF on real-world bimodal data obtained from simultaneous EEG and motion recordings. Motion was recorded using the inertial Xsens sensors which provided quaternion outputs. Subjects performed voluntary self-paced movements at random intervals, and they were asked to keep the minimum interval of 5 seconds. For each subject, four runs were recorded with resting periods of 3-4 minutes in between. Each run was 5 minutes long and included 25 trials on average. Moreover, EEG signals were recorded with a sampling frequency of 256Hz. The EEG electrodes were located as the common 10-20 systems, and we considered the central electrode (Cz) as the only predictor channel.

To generate a template of the RP wave, EEG signal was band-passed filtered from 0.1-4Hz and was segmented to trials according to the movement onsets². Then, trials were averaged to detect the RP in the test data using a matched filter. In order to obtain reliable results, the ROC curve was calculated by varying the detection threshold [7]. In this work, the final threshold was selected so that it provided a fixed FPR=2% with an average TPR=57%.

After selecting the parameters, the proposed IKF was compared with two KFs with different \mathbf{Q} covariance matrices selected via trial and error according to the variance of the rest and motion states. In order to assess the effect of SNR on the IKF behaviour, white Gaussian noise was added to the motion data to enable experiments with varying SNR from -20dB to 20dB. To evaluate the performance, the NRMS error was averaged over the entire test data. Fig. 5 illustrates the near-optimal performance of our proposed IKF for three subjects.

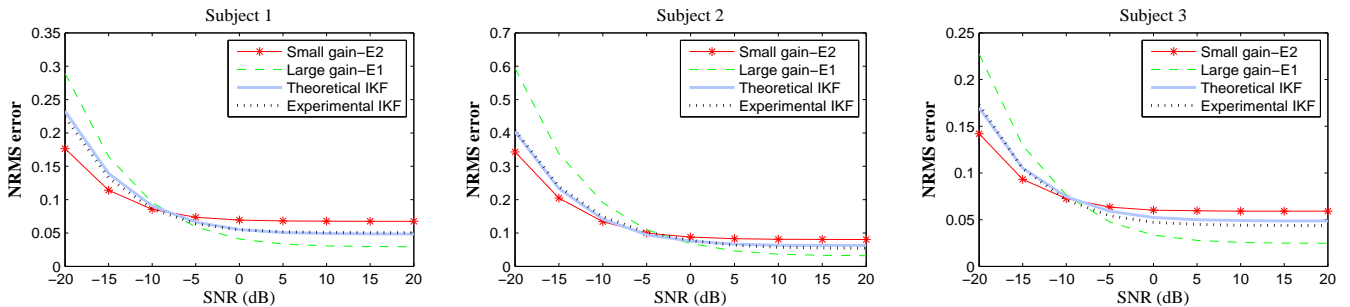


Fig. 5: Tracking the real motion data where online EEG has been used as the predictor channel. The error was averaged over 100 trials for an individual subject.

Remark#1: Note that experimental error in Fig. 5 was in agreement with the theoretical error derived in (1) considering the statistical measurement as FPR=2% with an average TPR=57%.

Remark#2: As expected, the IKF output was consistently superior than the worst scenario, i.e. it provided a near-optimal performance for both low and high SNR values. Observe that more reliable RP detection would improve the IKF performance.

Remark#3: In this work, we assume that noise process \mathbf{Q} was a preselected constant matrix. However, the concept of informed Kalman can be extended on iterative covariance estimation algorithms such as auto-covariance least square for further enhancement.

Remark#4: Unlike common signal processing driven diagnostic tools, we benefit from the available neurological information to improve the accuracy of our signal processing algorithm.

Remark#5: The EEG IKF method can be used as a potential filtering algorithm for motion tracking of patients with tremor in the rest state. Hence, it performs noise reduction in the steady state and it provides high responsiveness on the occurrence of voluntary movements.

Remark#6: Besides the above advantages, the proposed IKF requires an extrinsic channel which provides information about the state of the system. Thus, its application is limited to the systems which possess the predictor data. Furthermore, the performance of IKF is highly dependent on the detection accuracy of events in the predictor channel, i.e. a false state detection would affect the IKF behaviour.

5 CONCLUSION

Traditionally, state-based Kalman gain adaptation operates based on the observed measurements, whereas in this work gain adaptation is derived based on an extrinsic data channel which holds information on the state of the system. To this end, we have introduced a novel EEG informed Kalman algorithm (IKF) in which the physiological information has been exploited to

²Each onset was detected as the motion amplitude passed $\frac{1}{10}$ of its maximum in the current trial.

enhance the performance of the Kalman algorithm. For rigour, statistical and theoretical analysis have been provided to predict the performance of our proposed IKF, which was confirmed by simulation studies on both synthetic and real-world signals. Our proposed IKF achieved a near-optimal performance over a wide range of SNR, highlighting the consistency of our algorithm. In future, the concept of IKF can be introduced in multimodal applications such as in hybrid brain-computer-interface (hBCI) [11] to enhance the performance.

6 APPENDIX

6.1 Theoretical analysis

In this section, we seek to formulate the changes of Kalman gain in terms of the system characteristics. For simplicity, we consider³ $\mathbf{H} = \mathbf{F} = \mathbf{I}(4)$. Hence, the Kalman gain can be written as:

$$\mathbf{K}_0 = \mathbf{P}_{pr}(\mathbf{P}_{pr} + \mathbf{R})^{-1} = (\mathbf{P}_{up} + \mathbf{Q})(\mathbf{P}_{up} + \mathbf{Q} + \mathbf{R})^{-1} \quad (6)$$

As \mathbf{Q} and \mathbf{R} are directly included in the Kalman gain, changes of the gain can be calculated in terms of these covariance matrices. To this end, considering $\mathbf{A} = \mathbf{P}_{pr} + \mathbf{R}$, the Kalman gain is given by $\mathbf{K}_0 = \mathbf{P}_{pr}\mathbf{A}^{-1}$. Thus, changes of the Kalman gain can be represented as:

$$\mathbf{K}_n = \mathbf{K}_0 + \Delta\mathbf{K} = (\mathbf{P}_{pr} + \Delta\mathbf{P}_{pr})[\mathbf{A} + \Delta\mathbf{A}]^{-1} = (\mathbf{P}_{pr} + \Delta\mathbf{P}_{pr})[\mathbf{A}^{-1} - (\mathbf{I} + \mathbf{A}^{-1}\Delta\mathbf{A})^{-1}\mathbf{A}^{-1}\Delta\mathbf{A}\mathbf{A}^{-1}] \quad (7)$$

By substituting $\mathbf{A}^{-1} = \mathbf{P}_{pr}^{-1}\mathbf{K}$ it can be simplified as:

$$\mathbf{K}_n = (\mathbf{P}_{pr} + \Delta\mathbf{P}_{pr})[\mathbf{I} - (\mathbf{P}_{pr} + \mathbf{R} + \Delta\mathbf{A})^{-1}\Delta\mathbf{A}]\mathbf{P}_{pr}^{-1}\mathbf{K}_0 \quad (8)$$

where

$$\Delta\mathbf{A} = \Delta\mathbf{P}_{pr} + \Delta\mathbf{R} = [\Delta\mathbf{F}\mathbf{P}_{up}\Delta\mathbf{F}^T + \Delta\mathbf{Q}] + \Delta\mathbf{R} \quad (9)$$

Here we consider a constant measurement noise covariance for a specific set of experiment and therefore $\Delta\mathbf{R} = 0$. Furthermore, as the transition model is often unknown, we keep the initial state model matrix and try to compensate its changes through the process noise covariance. Thus $\Delta\mathbf{A} \approx \Delta\mathbf{Q}$ and (8) can be expressed as:

$$\mathbf{K}_n = (\mathbf{P}_{pr} + \Delta\mathbf{Q})[\mathbf{I} - (\mathbf{P}_{pr} + \mathbf{R} + \Delta\mathbf{Q})^{-1}\Delta\mathbf{Q}]\mathbf{P}_{pr}^{-1}\mathbf{K}_0 \quad (10)$$

in which adaptation of the Kalman gain is modelled in terms of the process noise. Similarly in Algorithm 1, for low variance state $\alpha = 0$, the Kalman gain is set to \mathbf{K}_2 which is generated from \mathbf{Q}_2 ; while for the higher variance state the gain is computed as $\mathbf{K}_n = \alpha\mathbf{K}_1 + (1 - \alpha)\mathbf{K}_2$ to cater for process noise covariance \mathbf{Q}_1 and \mathbf{Q}_2 .

REFERENCES

- [1] C. Jahanchahi and D. Mandic, "A class of quaternion Kalman filters," vol. 25, no. 3, pp. 533–544, 2014.
- [2] O. Šprdlík, Z. Hurák, M. Hoskovcová, O. Ulmanová, and E. Růžička, "Tremor analysis by decomposition of acceleration into gravity and inertial acceleration using inertial measurement unit," *Elsevier Biomed. Signal Process. and Contr.*, vol. 6, no. 3, pp. 269–279, 2011.
- [3] D. Choukroun, I. Y. Bar-Itzhack, and Y. Oshman, "Novel quaternion Kalman filter," vol. 42, no. 1, pp. 174–190, 2006.
- [4] A. Shmarlouski, Y. Shulhevich, S. Geraci, J. Friedemann, N. Gretz, S. Neudecker, J. Hesser, and D. Stsepankou, "Automatic artifact removal from GFR measurements," *Elsevier Biomed. Signal Process. Contr.*, vol. 14, pp. 30–41, 2014.
- [5] Z. Wang, J. Lam, and X. Liu, "Robust filtering for discrete-time Markovian jump delay systems," vol. 11, no. 8, pp. 659–662, 2004.
- [6] M. Efe, J. A. Bather, and D. P. Atherton, "An adaptive Kalman filter with sequential rescaling of process noise," *Proc. Amer. Contr. Conf.*, vol. 6, pp. 3913–3917, 1999.
- [7] D. L. Schomer and F. L. Da Silva, *Niedermeyer's electroencephalography: basic principles, clinical applications, and related fields*. Lippincott Williams & Wilkins, 2012.
- [8] H. Shibasaki and M. Hallett, "What is the Bereitschaftspotential?" *Elsevier Clin. Neurophysiol.*, vol. 117, no. 11, pp. 2341–2356, 2006.
- [9] S. Sanei, *Adaptive Processing of Brain Signals*. John Wiley and Sons, 2013.
- [10] I. K. Niazi, N. Jiang, O. Tiberghien, J. F. Nielsen, K. Dremstrup, and D. Farina, "Detection of movement intention from single-trial movement-related cortical potentials," *J. Neural Eng.*, vol. 8, no. 6, p. 066009, 2011.
- [11] R. Leeb, H. Sagha, R. Chavarriaga, and J. del R Millán, "A hybrid brain-computer interface based on the fusion of electroencephalographic and electromyographic activities," *Journal of neural engineering*, vol. 8, no. 2, p. 025011, 2011.

³Since the transition model is often unknown, any uncertainties in modelling can be captured in the noise covariances.